Virtual Synchronous Machine

F.J.N. Martins

***Abstract*—Synchronous generators rules the domain of power generation. Its characteristics guarantee stable Grid operation, damping, power compensating effect and voltage control.**

The concept of Virtual Synchronous Machine (VISMA) implements a control system in order to combine a three-phase inverter with synchronous generator behavior.

This study implements a Grid feeding system from a decentralized power source, using the VISMA connected to an infinite bus.

Results showed that VISMA has a damping effect around an equilibrium point and a compensator effect for Grid oscillations.

***Index Terms*—VISMA, Synchronous Machine, Symmetry Optimum Method, DSP, PI**

I. Introduction

Most of produced energy's converted in power plants by synchronous generators. These generators have many beneficial characteristics in electrical power grids, such as Grid's stability, damping around an equilibrium point for small disturbances and power compensator effect.

Virtual Synchronous Machine (VISMA) is an alternative method for electrical Grid feeding. Its concept consists in a three-phase inverter control system in such way it behaves as a synchronous generator, taking profit from the mentioned benefits of synchronous generators. This control system requires instantaneous grid voltage measurement to supply synchronous machine algorithm in a Digital Signal Processor (DSP) to determine instantaneous stator currents. To complete the cycle, the computed stator currents have to take effect at the Grid. For this purpose, a closed-loop current control system is implemented to drive inverter currents at the Grid.

II. Mathematical Modeling

Mathematical models need to be defined in order to run in DSP computer, using the per-unit system with the time expressed in seconds.

A. Synchronous Machine

This algorithm is implemented using Park's coordinate reference frame. Applying dq transformation to synchronous machine mathematical model provides a set of benefits: Constant self-inductance matrix, sinusoidal steady-state wave forms become constants and magnetically decoupled dq axis. This algorithm will be implemented considering two damper windings: one aligned to d axis, another aligned to q axis. Fig.1 represents Park's transformation applied to a synchronous machine, where d axis is aligned with the exciter winding:

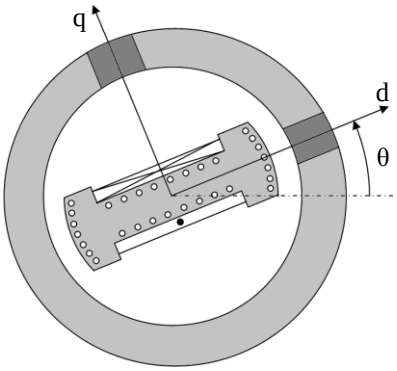

Fig. 1 – Application of Park's transformation to synchronous machines

DSP runs VISMA algorithm transforming Grid voltage data to dq coordinates using:

$$\begin{bmatrix} u_d \\ u_q \\ u_0 \end{bmatrix} = \mathbf{T} \begin{bmatrix} u_a \\ u_b \\ u_c \end{bmatrix} \tag{1}$$

With the following transformation matrix:

$$\mathbf{T} = \frac{2}{3} \begin{bmatrix} \cos(\theta) & \cos\left(\theta - \frac{2\pi}{3}\right) & \cos\left(\theta - \frac{4\pi}{3}\right) \\ -\text{sen}(\theta) & -\text{sen}\left(\theta - \frac{2\pi}{3}\right) & -\text{sen}\left(\theta - \frac{2\pi}{3}\right) \\ \frac{1}{2} & \frac{1}{2} & \frac{1}{2} \end{bmatrix} \tag{2}$$

Machine's currents are given by:

$$\begin{bmatrix} i_d \\ i_f \\ i_D \\ i_q \\ i_Q \end{bmatrix} = \begin{bmatrix} L_d & M_{df} & M_{Dd} & 0 & 0 \\ M_{df} & L_f & M_{Df} & 0 & 0 \\ M_{Dd} & M_{Df} & L_D & 0 & 0 \\ 0 & 0 & 0 & L_q & M_{Qq} \\ 0 & 0 & 0 & M_{Qq} & L_Q \end{bmatrix}^{-1} \begin{bmatrix} \Psi_d \\ \Psi_f \\ \Psi_D \\ \Psi_q \\ \Psi_Q \end{bmatrix} \tag{3}$$

Defining linkage fluxes as state variables [7]:

$$\Psi_d = \omega_b \int \left(u_d - R_s i_d + \omega_r \Psi_q\right) dt \tag{4}$$

$$\Psi_f = \omega_b \int (u_f - R_f i_f) dt \tag{5}$$

$$\Psi_D = -\omega_b \int R_D i_D \, dt \tag{6}$$

$$\Psi_q = \omega_b \int \left(u_q - R_s i_q - \omega_r \Psi_d\right) dt \tag{7}$$

$$\Psi_Q = -\omega_b \int R_Q i_Q \, dt \tag{8}$$

The inner torque is expressed in new variable terms:

$$T_{em} = \Psi_d i_q - \Psi_q i_d \tag{9}$$

Movement equation is obtained applying Newton's second law:

$$\omega_r = \frac{1}{2H} \int (T_{em} - T_c) \, dt \tag{10}$$

Rotor absolute angle is:

$$\theta = \int \omega_r \, dt \tag{11}$$

Response currents in abc coordinate are obtained applying inverse transform:

$$\begin{bmatrix} i_a \\ i_b \\ i_c \end{bmatrix} = \mathbf{T^{-1}} \begin{bmatrix} i_d \\ i_q \\ i_0 \end{bmatrix} \tag{12}$$

B. Three-phase inverter with low-pass RL filter

This converter is equipped with 6 IGBT devices with antiparallel connected diodes. In Fig.2 a three-phase inverter with a low-pass RL filter is represented:

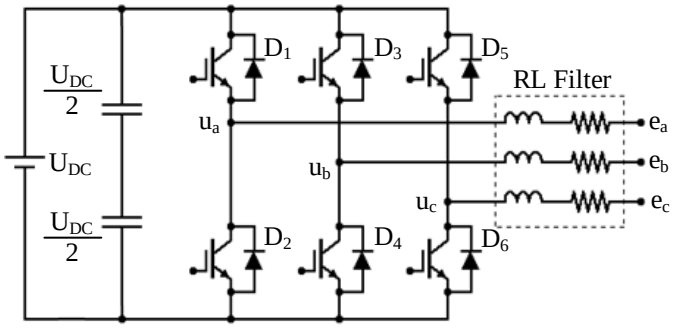

Fig. 2 – Three-phase inverter scheme

Three-phase inverter's transfer function is defined by a static gain with an associated delay. Mathematically, this delay is defined with time shift operator. However, a more convenient expression can be obtained using Taylor Series. Defining u_m as the modulating wave and u_{out} as the output voltage, thus [9]:

$$\frac{u_{out}}{u_m} = \frac{K_D}{1 + s\tau_D} \tag{13}$$

The inverter's transfer function is approximated to a first order system. Defining U_{DC}, u_c and T_{PWM} as DC voltage, carrier wave amplitude and PWM period, respectively, static gain and time constant from equation (13) are written in function of these parameters:

$$K_D = \frac{U_{DC}}{u_c} \tag{14}$$

$$\tau_D = \frac{T_{PWM}}{2} \tag{15}$$

As shown in Fig.2, RL low-pass filter connects inverter's output terminals to electrical Grid. Its transfer function is written in terms of internal resistance and inductance.

$$\frac{I(s)}{U(s)} = \frac{1}{\left(R + s\frac{L}{\omega_b}\right)} \tag{16}$$

According to Fig. 2, assuming ω_r as VISMA's virtual speed, from inverter's voltage equations in dq coordinates, currents expressions are obtained:

$$\begin{cases} i_d = \dfrac{u_d - e_d + \omega_r L i_q}{\left(s\frac{L}{\omega_b} + R\right)} \\ i_q = \dfrac{u_q - e_q - \omega_r L i_d}{\left(s\frac{L}{\omega_b} + R\right)} \end{cases} \tag{17}$$

The plant subsystem transfer function is the cascade combination from equations (13) and (17).

III. Current Control System

A. PI controllers

Controller subsystems are chosen in order to obtain the desired overall system dynamics. For this purpose, PI controllers are selected due to fast response and zero static error capacities.

PI controllers are defined with two terms: Proportional gain and Integral time constant:

$$K_p + \frac{K_i}{s} = K_p + \frac{K_p}{s\tau_i} = K_p\left(1 + \frac{1}{s\tau_i}\right) \tag{18}$$

System's diagram block is represented in Fig. 3:

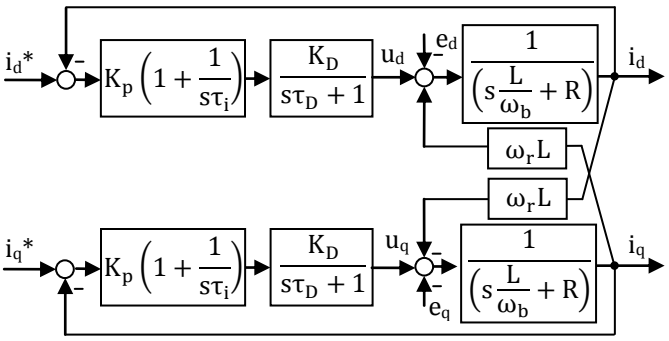

Fig. 3 – Current control system's block diagram

As shown in Fig. 3, current control system's coupled and exposed to disturbances.

B. *Symmetric Optimum Method*

Controller gains have a great importance in control system's performance, such as speed response, stability, regulation and overshooting.

Symmetric Optimum Method was designed to maximize phase margin, optimizing system's performance in the occurrence of disturbances and sudden changes in regulatory inputs. This Method establishes a pretended transfer function, adapting controller gains, so the equivalent dynamic system matches the desired transfer function.

Applying diagram block algebra to the dynamic system represented in Fig.3, considering R≈0, the following closed loop transfer function is obtained for i_d and i_q currents:

$$G(s) = \frac{sK_pK_D\tau_i + K_pK_D}{s^3\tau_i\tau_D L + s^2\tau_i L + s\tau_i K_pK_D + K_pK_D} \quad (19)$$

Applying Symmetric Optimum Method's general equation, optimized controller gains are given by:

$$\begin{cases} \tau_i = 4\tau_D \\ K_p = \dfrac{L}{2K_D\tau_D\omega_b} \end{cases} \quad (20)$$

IV. Experimental Implementation

To implement synchronous machine algorithm and current control system, Data Acquisition Boards (DAB) are required to instantaneously measure Grid voltage and inverter's phase currents. For this purpose, two DAB were designed: voltage and current measurement boards, equipped with voltage and current transducers, respectively. This data is converted to digital format by an Analog-to-Digital converter embedded in DSP. Fig.4 represents the experimental set up scheme:

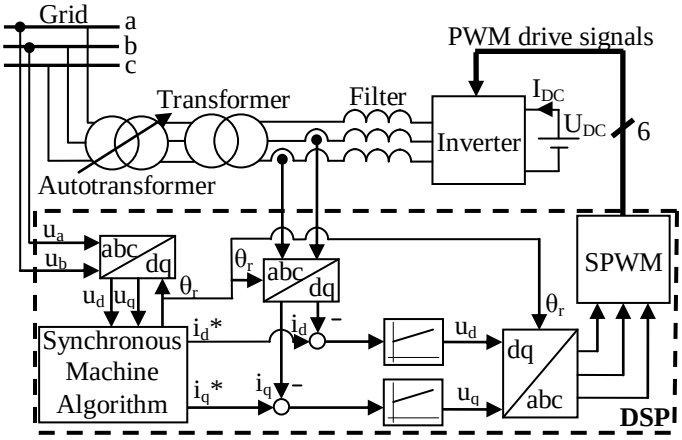

Fig. 4 – Experimental set up scheme

The current control system will be implemented using per-unit system, which base values are represented in Table I:

TABLE I
PER UNIT SYSTEM

Symbol	Description	Base Value
U_b [V]	Grid Voltage	400
U_{Tb} [V]	Output Voltage	70
U_{DCb} [V]	DC link Voltage	200
ω_b [rad/s]	Angular Speed	100π
I_b [A]	Output Current	5
L_b [H]	Induction	0,0446

The components' characteristics used in laboratory and gain values are exposed in Table II:

TABLE II
COMPONENTS' CHARACTERISTICS AND GAINS

Symbol	Description	Value	Value p.u.
L	Low-pass filter inductance	0,015 [H]	0,336
R	Low-pass filter resistance	0,8 [Ω]	0,057
U_T	Transformer's voltage	70 : 400 [V]	1:1
f_{PWM}	PWM frequency	6000 [Hz]	---
τ_D	Inverter time constant	83,3 [μs]	---
K_D	Inverter static gain	20,5	---
u_c	Carrier wave amplitude	0,0745	---
τ_i	Integral time constant	0,333 [ms]	---
K_p	Proportional Gain	0,3135	---
K_i	Integral Gain	941	---

V. Results

A. *Closed-Loop Current control*

This test verifies the performance of current control system, analyzing time response and overshooting.

For an easier analysis, it will be introduced step regulatory currents separately: First it's introduced a step in i_d*=1p.u. while i_q*=0p.u.

Results are shown in Fig.5:

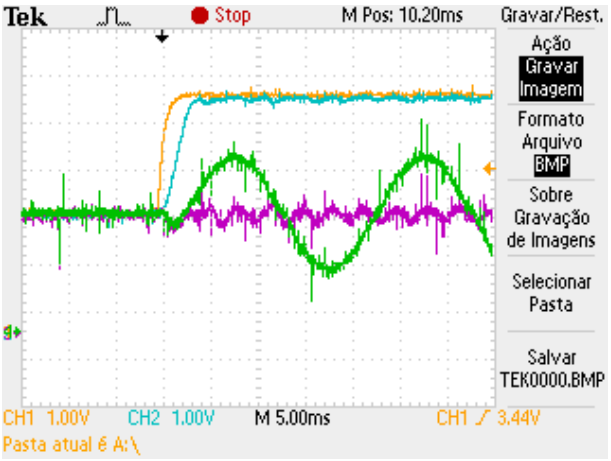

Fig. 5 – Time responses: i_d* (yellow; 0,4 p.u./div), i_d (blue; 0,4 p.u./div), i_q (purple; 0,4 p.u./div), i_a (green, 0,8p.u./div)

In the second test, regulatory currents are set to i_d*=0p.u. while i_q*=1p.u. Results are represented in Fig.6:

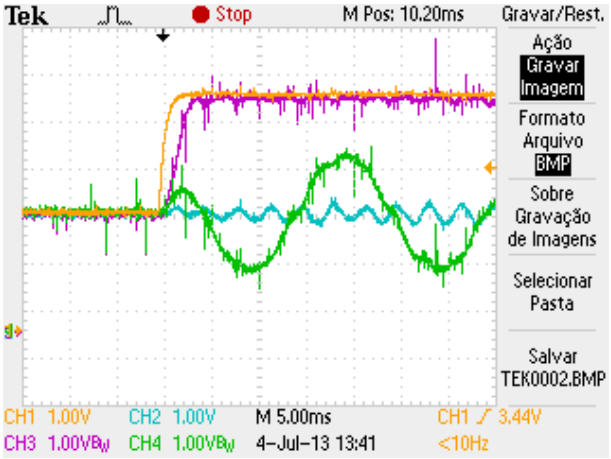

Fig. 6 – Time responses: i_q* (yellow; 0,4 p.u./div), i_d (blue; 0,4 p.u./div), i_q (purple; 0,4 p.u./div), i_a (green, 0,8p.u./div)

Current control system has a time response of approximately 4 ms, which is a fast response relatively to Grid's wave period (20 ms). Results show that there's no significant overshooting in output currents and controllers can decouple i_d and i_q components.

B. *Virtual Synchronous Machine*

In this test, regulatory currents are generated from VISMA algorithm. To this end, generator's parameters must be defined to run the algorithm in DSP. Table III shows the emulated virtual generator's parameters:

TABLE III
VIRTUAL SYNCHRONOUS MACHINE PARAMETERS

Symbol	Description	Value
X_d [p.u.]	Synchronous Reactance d axis	0,85
X_{ls} [p.u.]	Stator dispersion	0,12
X_{md} [p.u.]	Mutual inductance in d axis	0,73
X_q [p.u.]	Synchronous Reactance q axis	0,48
X_{mq} [p.u.]	Mutual inductance in d axis	0,36
X_f [p.u.]	Field inductance	0,2049
X_{kd} [p.u.]	Damping winding inductance in d axis	0,16
X_{kq} [p.u.]	Damping winding inductance in q axis	0,1029
R_a [p.u.]	Stator resistor	0,1
R_f [p.u.]	Field resistor	0,02
R_D [p.u.]	Damping winding resistor in d axis	0,0204
R_Q [p.u.]	Damping winding resistor in q axis	0,0212
u_f [p.u.]	Field voltage	0,007
H [s]	Inertia Constant	0,1

In this experimental implementation, the differential equations are solved using Heun's numerical integration method.

1) *Paralel connection test*

To connect a synchronous generator to an electrical Grid, there are a few conditions required: Synchronous speed, same phase voltage magnitude, position and sequency. For this purpose, VISMA is initially set to have a virtual speed aproximately equal to Grid frequency. DSP is programmed to connect VISMA authonomously to electrical Grid when all connection conditions are verifyed. Transient stator currents due to paralel connection are represented in Fig. 7:

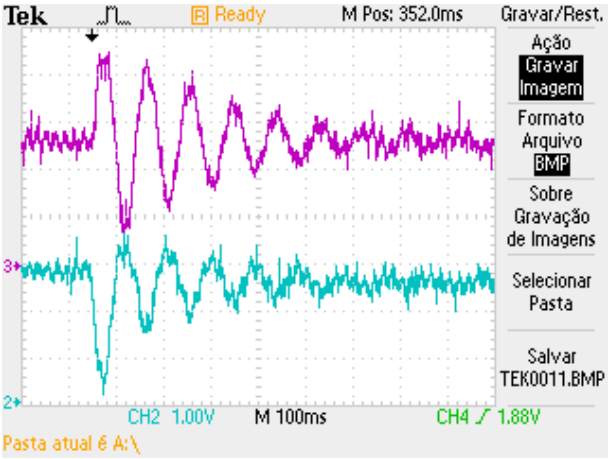

Fig. 7 – Connection Transient: i_d*(blue; 0,4 p.u./div), i_q*(purple; 0,4p.u./div)

Fig. 7 shows that currents i_d* and i_q* have a damping effect that tends to a no-load steady state. Fig. 8 displays VISMA in this final steady state:

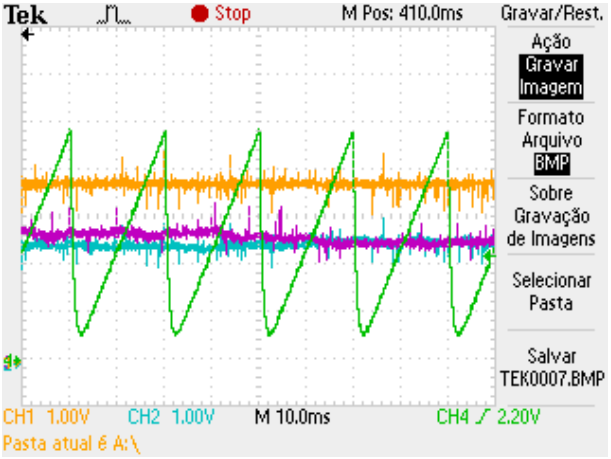

Fig. 8 – VISMA in steady state, no load regime: i_d*(blue; 0,4 p.u./div), i_q*(purple; 0,4p.u./div), ω_r (yellow; 0,8p.u./div), θ (green; 0,5p.u./div)

In steady state, speed is practically constant and stator currents are null. Rotor's angle has a synchronous waveform (T=20ms) and its representation was adjusted so the upper limit corresponds to π radians and the lower limit $-\pi$ radians.

2) *Exciter influence in stator currents*

In the previous test, VISMA was set with a field current corresponding to no-load conditions (u_f =0,007p.u.). In this test, field voltage will be increased with a step to u_f = 0,0105p.u. Results are represented in Fig. 9.

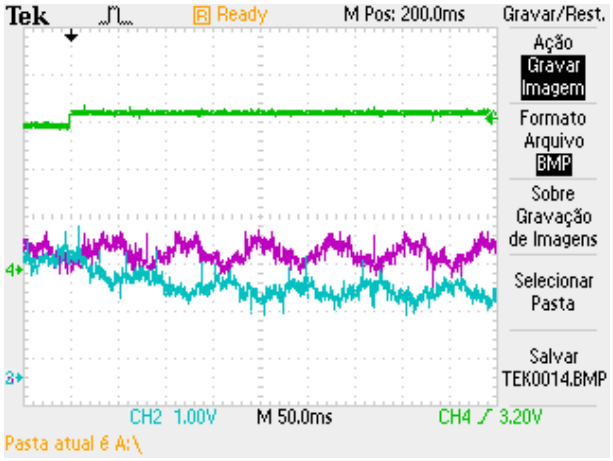

Fig. 9 – Field voltage step: u_f(green; 3,2p.u./div), i_d*(blue; 0,4p.u./div), i_q*(purple; 0,4 p.u./div)

When field voltage is increased, field current will proportionally increase in function of the field resistor. Consequently, the linkage flux in d axis will grow, and VISMA leaves the no load condition, due to the i_d* current, which is associated to reactive power injection. From this point forward, all tests will have a field voltage of u_f = 0,0105p.u. as initial conditions.

3) Load test

In this test, a sudden torque is applied in software to virtual synchronous machine's shaft. The stator currents will have a transient regime tending to a load operating point, where the inner torque equals the load torque. Fig. 9 shows stator currents and torque temporal evolutions for a step input in load torque with a magnitude of 0,4 p.u.:

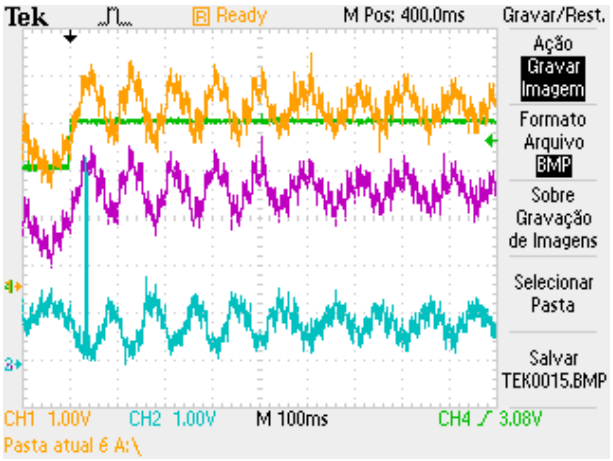

Fig. 10 – Load torque step from a no load operating point: i_d*(blue; 0,4 p.u./div), i_q*(purple; 0,4p.u./div), T_c (green; 0,4 p.u./div), T_{em} (yellow; 0,4 p.u./div)

Inner torque has a damping around the equilibrium point (load torque). Both currents tend to non zero values, corresponding to a load operating point.

4) Compensating effect test

In this experiment, a sudden voltage drop of 20% in Grid's voltage will be introduced in software to verify VISMA's compensating effect for Grid disturbances:

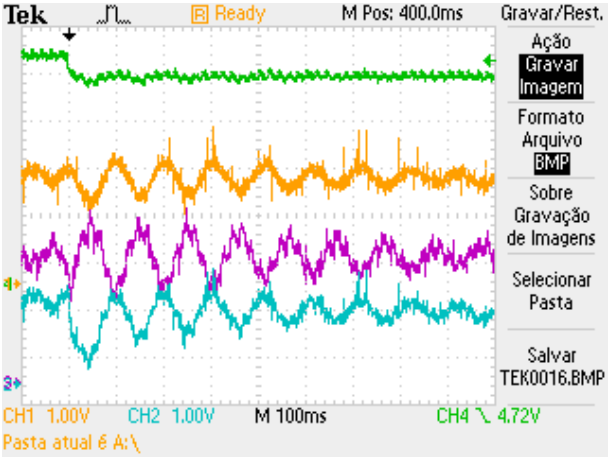

Fig. 11 – Sudden voltage: u_d(yellow; 0,4p.u./div), u_q(green, 0,4p.u./div), i_d*(blue; 0,8p.u./div), i_q*(0,8p.u./div)

VISMA has an immediate response in currents i_d* and i_q* with a damping oscillating dynamics. i_q* tends to a zero value, while i_d* has a non zero final value. This means that in steady state, VISMA will feed the electrical grid with reactive power exclusively.

VI. Conclusion

Symmetry Optimum Method applied to current control system provides fast response, no significant overshooting and zero steady state error.

In VISMA's implementation, there were several problems observed: Initially, differential equations were solved using Euler's Method that leaded the system to instability due to mathematical divergence, which encouraged the use of Heun's integration Method. With this Method, VISMA's algorithm presented satisfactory results. One other pointed out problem is the diversity of numerical values associated to a synchronous generator, even with the use of per-unit system, numerical representation can be conditioned due to DSP architecture. In these experiments, a 16 bit microprocessor was used with two's complement numerical representation, which wasn't sufficient to introduce the desired inertia constant and exciter winding parameters.

What concerns VISMA's performance, it was shown that virtual synchronous machine have an immediate response for Grid disturbances, generating stator current waveforms entirely as a synchronous machine. However, current control system wasn't implemented because it was considered irrelevant the effect of a VISMA feeding an infinite bus. In future studies, experiments in isolated electrical grids using VISMA are appropriate to study its compensating effect in the occurrence of Grid disturbances.

REFERENCES

[1] J. P. S. Paiva, "Redes de Energia Eléctrica – Uma Análise Sistémica", IST Press, 2011

[2] "Generator Grid Connection Guide V2", Westernpower, 2011

[3] Y. Chen, R. Hesse, D. Turschner and H. Beck, *"Dynamic Properties of the Virtual Synchronous Machine"*, Institute of Electrical Power Engineering, Clausthal, Germany

[4] R. Hesse, D. Turschner and H. Beck, "*Micro grid stabilization using the Virtual Synchronous Machine*", Institute of Electrical Power Engineering, Clausthal, Germany

[5] G. Marques, "Dinâmica das Máquinas Eléctricas", Instituto Superior Técnico, 2007.

[6] G. Marques, "Controlo de Motores Eléctricos", Instituto Superior Técnico, 2007

[7] J. C. P. Palma, Accionamentos Electromecânicos de Velocidade Variável, Fundação Calouste Gulbenkian, 2008

[8] J. F. Silva, "Sistemas de Conversão Comutada: Semicondutores e Conversores Comutados de Potência", Instituto Superior Técnico, 2012

[9] A. Jorge, "Estudo e implementação Experimental de Conversores AC/DC de Onda Sinusoidal" – Dissertação para Obtenção de Grau de Mestre, Instituto Superior Técnico, 2009

[10] D. Carreira, "Desenvolvimento de um Sistema de Armazenamento de Energia Híbrido" – Dissertação para Obtenção de Grau de Mestre, Instituto Superior Técnico, 2012

[11] S. Preitl, R. Precup, "Points of View In Controller Design by Means of Extended Symmetrical Optimum Method", "Politehnica" University of Timisoara, Romania

[12] Mizera, Roman, "Modification of Symmetric Optimum Method", XXX. ASR 2005 Seminar, Instruments and Control, Ostrava, April 29, 2005.

[13] P.C. Krause, O.Wasynczuk, S. D. Sudhoff – "Analysis of Electric Machinery and Drive Systems", IEEE press, 2002

[14] J. Santana, "Conversores Comutados para Energias Renováveis", Instituto Superior Técnico, 2012

[15] MICROCHIP®, "dsPIC30F4011/4012 Datasheet", MICROCHIP Technology Inc, 2008 (http://www.microchip.com)

[16] MICROCHIP®, "Using MPLAB ICD 2 Poster" - MICROCHIP Technology Inc, 2004 (http://www.microchip.com)

[17] MICROCHIP®, "dsPIC30F Family Reference Manual", MICROCHIP Technology Inc, 2005

[19] LEM®, "Voltage Transducer LV 25-P datasheet", 2012 (http://www.lem.com)

[20] LEM®, "Current Transducer LTSR 25-NP datasheet", 2012 (http://www.lem.com)